

Altered amplitude of low-frequency fluctuations and default mode network connectivity in high myopia: a resting-state fMRI study

Xue-Wei Zhang^{1,2}, Rong-Ping Dai³, Gang-Wei Cheng³, Wei-Hong Zhang¹, Qin Long³

¹Department of Radiology, Translational Medical Center, Peking Union Medical College Hospital, Chinese Academy of Medical Sciences & Peking Union Medical College, Beijing 100730, China

²Department of Interventional Radiology, Emergency General Hospital, Beijing 100028, China

³Department of Ophthalmology, Translational Medical Center, Peking Union Medical College Hospital, Key Laboratory of Ocular Fundus Diseases, Chinese Academy of Medical Sciences & Peking Union Medical College, Beijing 100730, China

Co-first authors: Xue-Wei Zhang and Rong-Ping Dai

Correspondence to: Qin Long and Wei-Hong Zhang. Shuaifuyuan Road, Beijing 100730, China. longqinbj@hotmail.com; wehong2007@gmail.com

Received: 2019-12-19 Accepted: 2020-07-09

Abstract

• **AIM:** To analyze changes in amplitude of low-frequency fluctuations (ALFFs) and default mode network (DMN) connectivity in the brain, using resting-state functional magnetic resonance imaging (rs-fMRI), in high myopia (HM) patients.

• **METHODS:** Eleven patients with HM (HM group) and 15 age- and sex-matched non-HM controls (non-HM group) were recruited. ALFFs were calculated and compared between HM group and non-HM group. Independent component analysis (ICA) was conducted to identify DMN, and comparisons between DMNs of two groups were performed. Region-of-interest (ROI)-based analysis was performed to explore functional connectivity (FC) between DMN regions.

• **RESULTS:** Significantly increased ALFFs in left inferior temporal gyrus (ITG), bilateral rectus gyrus (REC), bilateral middle temporal gyrus (MTG), left superior temporal gyrus (STG), and left angular gyrus (ANG) were detected in HM group compared with non-HM group (all $P < 0.01$). HM group showed increased FC in the posterior cingulate gyrus (PCC)/precuneus (preCUN) and decreased FC in the left medial prefrontal cortex (mPFG) within DMN compared with non-

HM group (all $P < 0.01$). Compared with non-HM group, HM group showed higher FC between mPFG and bilateral middle frontal gyrus (MFG), ANG, and MTG (all $P < 0.01$). In addition, HM patients showed higher FC between PCC/(preCUN) and the right cerebellum, superior frontal gyrus (SFG), left preCUN, superior frontal gyrus (SFG), and medial orbital of the superior frontal gyrus (ORB supmed; all $P < 0.01$).

• **CONCLUSION:** HM patients show different ALFFs and DMNs compared with non-HM subjects, which may imply the cognitive alterations related to HM.

• **KEYWORDS:** functional magnetic resonance imaging; high myopia; default mode network; amplitude of low-frequency fluctuation

DOI: 10.18240/ijo.2020.10.18

Citation: Zhang XW, Dai RP, Cheng GW, Zhang WH, Long Q. Altered amplitude of low-frequency fluctuations and default mode network connectivity in high myopia: a resting-state fMRI study. *Int J Ophthalmol* 2020;13(10):1629-1636

INTRODUCTION

The prevalence of high myopia (HM), a common eye disorder, has increased dramatically in the past decades, worldwide, especially in Asia^[1-2]. HM represents a refractive error below -6 diopter (D), and predisposes the eye to various pathologic changes involving the sclera, choroid, and retina, which can result in visual impairment and blindness^[3-4]. Recently, functional connectivity density (FCD) mapping and seed-based correlation analyses showed that HM causes FCD and morphological changes in the brain^[5-6], implying a link between HM and cognitive dysfunction^[7-9]. In addition, a public health study involving more than a million adolescents suggested that cognitive function is highly correlated with HM^[10]. However, the neural characteristics, especially the cognitive alterations, associated with HM patients have not been clarified.

Resting-state functional magnetic resonance imaging (rs-fMRI), which measures brain activity by detecting changes in blood flow during activity compared with the resting state, has been widely used to explore cognitive characteristics^[11-12].

Table 1 Subjects' characteristics

Characteristics	HM group (<i>n</i> =11)	Non-HM group (<i>n</i> =15)	<i>t</i> / χ^2 test	<i>P</i>
Age, mean \pm SD	50.2 \pm 13.7	48.2 \pm 12.2	0.3897	0.7002
Sex, M/F	3/8	5/10	0.1094	0.7408
Handedness, R/L	10/1	14/1	0.0525	0.8187
Mean SE, R/L	-13.98/-12.08	0.21/0.20	10.51/10.96	<0.0001/<0.0001

SE: Spherical equivalent; R: Right; L: Left. *t*-test for comparing age and SE of two groups; χ^2 test for comparing sex and Handedness of two groups.

One valuable index that can be measured during rs-fMRI is the amplitude of low-frequency fluctuations (ALFFs), which reflect spontaneous neural activity^[13-14]. In addition, the default mode network (DMN), which comprises the posterior cingulate cortex (PCC), medial prefrontal cortex (mPFC), and bilateral parietal cortices, has been found to be altered during cognitive impairment and neurodegeneration^[15-16]. To date, neuroimaging studies examining the spontaneous neural activity and functional cognitive changes that occur in HM patients have been inadequate.

The purpose of this study was two-fold: first, to analyze the ALFFs and DMN connectivity in HM patient brain using rs-fMRI; and second, to explore the distribution of anomalous regional intrinsic activities in the HM brain by performing independent component analysis (ICA) and region-of-interest (ROI) analyses, to evaluate the inter-regional functional connectivity (FC) among DMN regions. We hypothesized that HM patients may have different ALFFs and DMNs than non-HM subjects, which may be associated with cognitive alterations caused by HM.

SUBJECTS AND METHODS

Ethical Approval All protocols were approved by a local ethics committee and were performed in accordance with the Declaration of Helsinki, and full written consent was obtained from all participants.

Subjects Unrelated Chinese patients, either with or without HM, were recruited from the Department of Ophthalmology, Peking Union Medical College Hospital.

Eleven patients with HM (HM group), who had spherical equivalents (SEs) of at least -6.00 D in both eyes and appropriately corrected by wearing glasses, were recruited, and 15 emmetropic age- and sex-matched individuals (non-HM group), with SEs within ± 1.0 D in both eyes, served as the control group for this study (Table 1). Participants were excluded from the current study for diagnoses of ocular disorders other than HM, medical, neurological, or psychiatric illnesses, use of alcohol, caffeine, or nicotine within the last 3mo, and any magnetic resonance imaging (MRI) contraindications.

Magnetic Resonance Imaging Data Acquisition All images were acquired with a 3-T MRI scanner (MAGNETOM Skyra, Siemens, Erlangen, Germany). We obtained 200 functional

images using the echo-planar imaging sequence with the following parameters, repetition time (TR)=2510ms, echo time (TE)=3ms, slice thickness=3 mm, gap=0 mm, field of view (FOV)=240 \times 240 mm², acquisition matrix=80 \times 80, flip angle=90°. In addition, T1-weighted high-resolution structural images were obtained using the gradient-echo sequence with the following parameters, TR=2300ms, TE=3.17ms, TI=900ms, slice thickness=1 mm, gap=0 mm, FOV=256 \times 256 mm², acquisition matrix=256 \times 256, flip angle=8°. Earphones and earplugs were used to reduce acoustic noise. For the resting state scan, all subjects were required to remain still with their closed eyes, and instructed not to think about anything special or fall sleep.

Functional Magnetic Resonance Imaging Data Preprocessing All rs-fMRI and structural data preprocessing was achieved by Data Processing Assistant for Resting-State fMRI (DPARSF) based on some functions in Statistical Parametric Mapping (SPM8, <http://www.fil.ion.ucl.ac.uk/spm/software/spm8/>) and Resting-State fMRI Data Analysis Toolkit 1.8 (REST). Preprocessing includes the following steps, 1) the first 10 points of the rs-fMRI for every subjects were discarded to maintain data stabilization; 2) slice-timing correction, head-motion correction, and nuisance covariate removal were performed. During the preprocessing, if the subjects' head motions indicated rotations exceeding 2.5° or 2.5 mm in the X-, Y-, or Z-axis, the subjects were excluded. No participants in this study were excluded due to head motion; 3) rs-fMRI data were normalized to the Montreal Neurological Institute (MNI) space by the method of unified segmentation on the T1-weighted image, and resampled to a 3-mm³ cube voxel; 4) these images were smoothed with the Gaussian smoothing kernel of 6 \times 6 \times 6 mm³. After smoothing, linear detrending, temporally band-pass filtering (typical band: 0.01-0.08 Hz), and the removal of nuisance covariates were performed.

The Amplitude of Low-Frequency Fluctuation Analysis The ALFF value was obtained by using the DPARSF software with the following steps. The power spectrum was obtained by using a fast Fourier transform, which converted the time series of each voxel into a frequency domain. The square root of the power spectrum (typical band: 0.01 to 0.08 Hz) was called ALFF. Then, the global mean ALFF was used for further analysis.

Independent Component Analysis We performed the Subject Order Independent Group ICA (SOI-GICA)^[17], which was based on the group ICA (GICA) function of the functional magnetic resonance imaging (fMRI) toolbox (Stable and Consistent Group ICA of the fMRI Toolbox, version 1.2; <http://www.nitrc.org/projects/cogicat/>). SOI-GICA includes the following three advantages, which were multiple times, randomized initial values and different subject orders. We performed SOI-GICA with the following major parameters (GICA 100 times and 20 independent components). Eight significant components were identified as resting-state networks (RSNs) by visual observation. The individual-level components were acquired and transformed into z-scores, which belong to Gaussian distributions.

Independent component patterns representing RSNs were analyzed by using a one-sample Student's *t*-test ($t > 15$) to better display each brain network. A two-sample Student's *t*-test was used to compare the differences within DMNs between HM patients and non-HM controls. AlphaSim correction was conducted to result in a corrected threshold of $P < 0.01$ [AlphaSim program in REST software, Major parameters: single voxel $P = 0.01$, 1000 simulations, full-width at half maximum (FWHM) = 6 mm, cluster connectivity criterion = 5 mm].

Default Mode Network Connectivity Analysis FC between ROIs, based on the ICA findings within voxels of the whole brain, was calculated. The time courses of ROIs in both groups were extracted. Pearson correlation analysis between the time course of ROIs and that of every voxel in the whole brain was computed to obtain a map of correlation coefficients. The resultant values were converted to a map of Gaussian distributed values, using Fisher's z-transformation, resulting in z-FC maps. One-sample Student's *t*-tests were performed on the non-HM group's z-FC maps to identify the normal network. Two sample Student's *t*-tests were then performed to compare the z-FC maps between HM patients and healthy controls. Corrected cluster thresholds were determined by using Monte Carlo simulations (AlphaSim program in REST software). A cluster connection radius of 5 mm, FWHM = 6 mm, and a height threshold of $P < 0.01$ were achieved for FC analyses. Brain regions with altered FC were projected onto a three-dimensional ICBM152 smoothed-brain, using BrainNet Viewer software.

Statistical Analysis Group comparisons of data were achieved by using a χ^2 test, for categorical variables, and Student's *t*-tests, for continuous variables, using the Statistical Package for the Social Sciences version 19.0 (SPSS, Chicago, IL, USA). After preprocessing, the functional data were all in accordance with normal distribution through Fourier transform. $P < 0.01$ was considered statistically significant.

Table 2 Regions showing ALFF differences between HM group and non-HM group

Brain areas	BA	Voxels	MNI coordinates, mm			<i>t</i> value for peak voxels
			x	y	z	
L ITG	20	36	-42	-27	-27	6.2864
R REC	11	18	3	24	-24	4.8824
L REC	11	45	-3	57	-21	5.5339
R MTG	21	13	69	-21	-6	4.7061
R MTG	21	21	54	-39	0	5.1903
L STG	22	14	-60	-27	12	5.2146
L ANG	39	31	-45	-51	27	6.7717

ITG: Inferior temporal gyrus; REC: Rectus gyrus; MTG: Middle temporal gyrus; STG: Superior temporal gyrus; ANG: Angular gyrus; R: Right; L: Left; BA: Brodmann area; MNI: Montreal Neurological Institute.

Table 3 Differences in the DMN between HM group and non-HM group

Brain areas	BA	Voxels	MNI coordinates, mm			<i>t</i> value for peak voxels
			x	y	z	
L mPFG	9	83	-3	42	36	-4.7479
R PCC/preCUN	23	35	15	-48	36	4.5272

mPFG: Medial prefrontal gyrus; PCC: Posterior cingulate cortex; preCUN: Precuneus; R: Right; L: Left; BA: Brodmann area; MNI: Montreal Neurological Institute.

RESULTS

Amplitude of Low-Frequency Fluctuation Differences Between HM Group and Non-HM Group The ALFFs of all participants during the resting state were analyzed. Compared with the non-HM group, the ALFF values in the HM group increased in the left inferior temporal gyrus (ITG), bilateral rectus gyrus (REC), right middle temporal gyrus (MTG), left superior temporal gyrus (STG), and left angular gyrus (ANG) (two-sample Student's *t*-test, AlphaSim corrected, $P < 0.001$, 13 voxels; Table 2, Figure 1).

Functional Connectivity Differences in the Default Mode Networks Between the HM Group and the Non-HM Group The DMNs were extracted from each subject by manual operation. FC data was based on the correlations between a seed region and voxels within the brain. In this study, the HM group showed increased FC in the PCC/precuneus (preCUN) and decreased FC in the left mPFC compared with the non-HM group (two-sample Student's *t*-test, $P < 0.01$; Table 3, Figure 2).

ICA and DMN Connectivity Analysis The PCC/preCUN and medial prefrontal gyrus (mPFG), determined by ICA findings, were extracted as ROIs, using the rs-fMRI Data Analysis Toolkit (REST). Significant differences were noted in the Z-FC maps for the resting state between the HM group and the non-HM group (two-sample Student's *t*-test, $P < 0.01$,

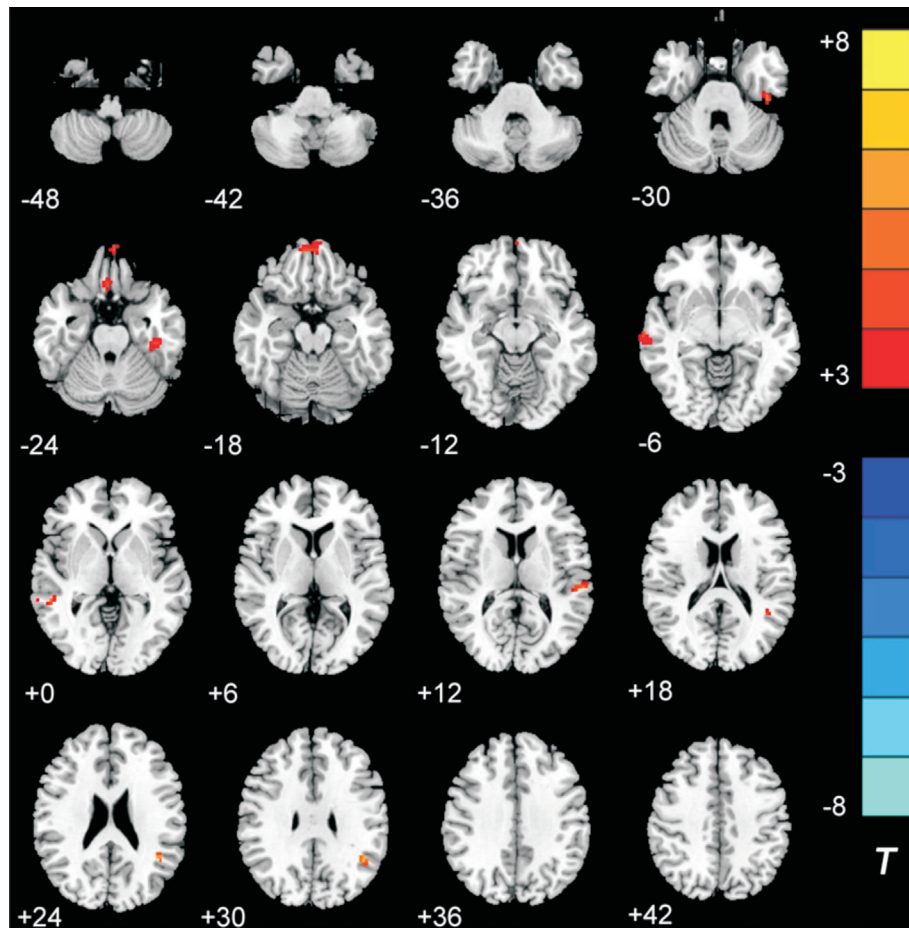


Figure 1 ALFF differences between HM patients (HM group) and non-HM control subjects (non-HM group) Compared with the values in the non-HM group, the ALFF values in HM patients increased in the left ITG, bilateral REC, right MTG, left STG, and left ANG (marked with red dots). The threshold was set at $P < 0.001$ (AlphaSim corrected, $P < 0.001$, 13 voxels).

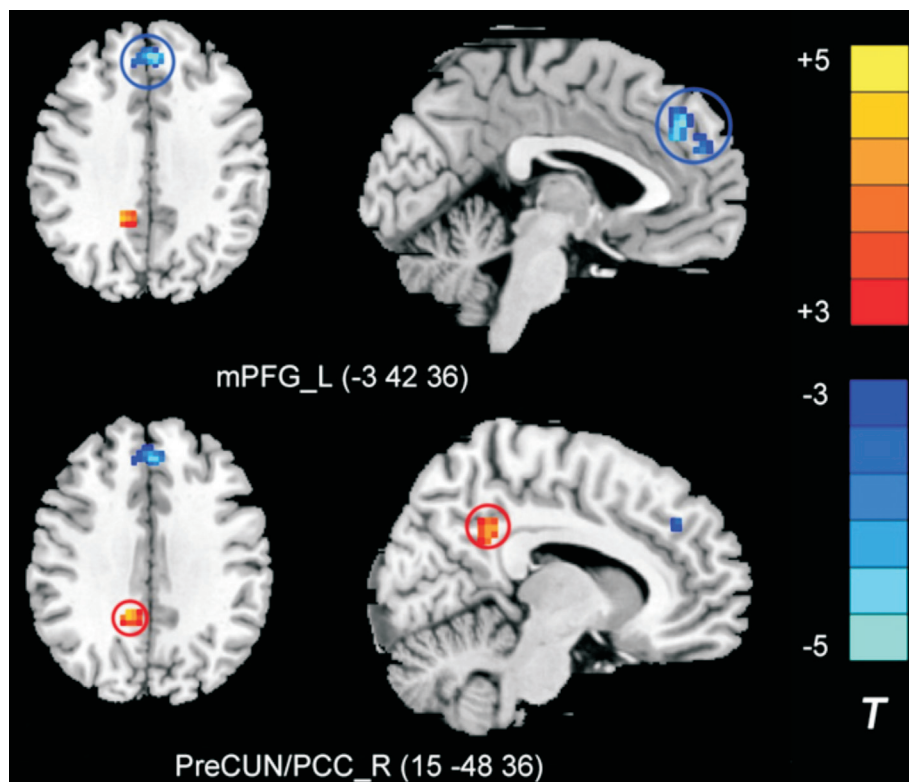


Figure 2 FC differences in DMNs between HM patients (HM group) and non-HM control subjects (non-HM group) The HM group showed increased FC in the PCC/preCUN (marked with red dots) and decreased FC in the left mPFG compared with the values for the non-HM group (marked with blue dots). The threshold was set at $P < 0.01$ (AlphaSim corrected, $P < 0.01$, 30 voxels).

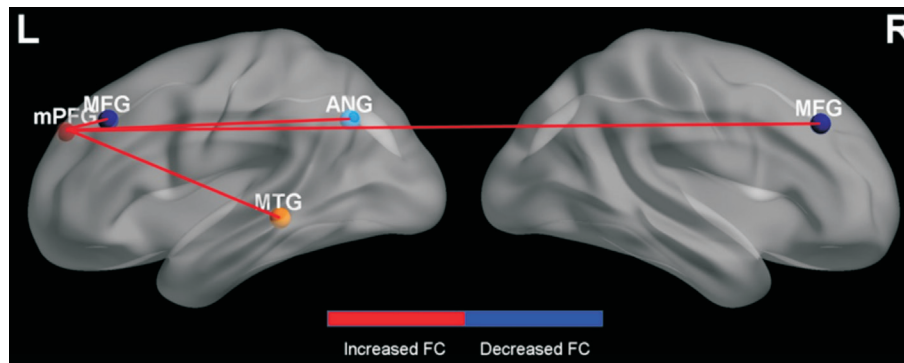


Figure 3 A 3D map displaying the increased and decreased FC of ROIs between HM patients (HM group) and non-HM controls (non-HM group) All of the regions with increased FC for ROIs between the two groups were connected by red lines (right MFG, left MFG, ANG, and MTG), whereas all of the regions with decreased FC for ROIs between the two groups were connected by blue lines (None).

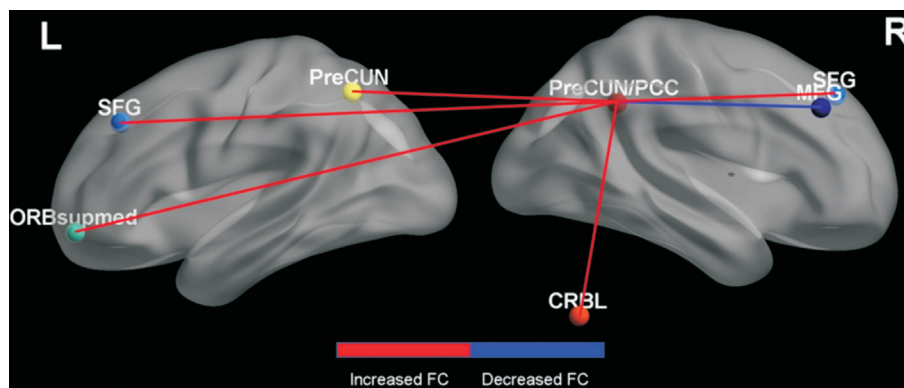


Figure 4 FC for regions-of-interest (ROIs) between HM patients (HM group) and non-HM controls (non-HM group) All of the regions with increased FC for ROIs between the two groups were connected by red lines (right CRBL and SFG, left preCUN, SFG, and ORB supmed), whereas all of the regions with decreased FC for ROIs between the two groups were connected by blue lines (right MFG).

Table 4 Altered FC of ROIs between HM group and non-HM group

Brain areas	BA	Voxels	MNI coordinates, mm			<i>t</i> value for peak voxels
			x	y	z	
L MTG	21	59	-60	-36	-9	5.6144
L ANG	39	67	-42	-51	30	5.5303
R MFG	46	62	30	18	36	5.0265
L MFG	46	75	-36	21	42	4.471

MTG: Middle temporal gyrus; MFG: Middle frontal gyrus; ANG: Angular gyrus; R: Right; L: Left; MNI: Montreal Neurological Institute; BA: Brodmann area.

AlphaSim corrected; Figures 3 and 4). Compared with the non-HM group, the HM group showed higher FC between the mPFG and the right middle frontal gyrus (MFG), left MFG, ANG, and MTG ($P < 0.01$; Figure 3, Table 4). In addition, the HM group showed increased FC between the PCC/preCUN and the right cerebellum (CRBL) and superior frontal gyrus (SFG), left preCUN, SFG, and medial orbital of the superior frontal gyrus (ORB supmed) and decreased FC between the PCC/preCUN and the right MFG compared with the non-HM group ($P < 0.01$; Figure 4, Table 5).

DISCUSSION

In our study, HM patients showed altered ALFFs and DMNs compared with non-HM subjects, which may imply cognitive

alterations associated with HM. Different from previous fMRI studies which applied voxel-based analysis, such as ALFF^[18-19], degree centrality^[20] and FCD^[5], we combined voxel-based analysis with ICA to detect changes of spontaneous brain activity and alternations of DMN in HM group from the view of cerebral functional dissociation and integration.

ALFF values, which represent spontaneous neural activity, were significantly increased in the left ITG, left STG, left ANG, right MTG, and bilateral REC of the HM group compared with those of the non-HM group, in our study. As part of the ventral stream, the ALFFs in the ITG may reveal visual stimuli processing, object identification, and memory recall and can be modulated by attention to stimuli^[21-22]. Decreased ALFF values

Table 5 Altered FC of ROIs between HM group and non-HM group

Brain areas	BA	Voxels	MNI coordinates, mm			<i>t</i> value for peak voxels
			x	y	z	
R CRBL	-	47	36	-66	-45	3.4625
ORB supmed	10	197	-3	51	-6	4.2194
R MFG	10	44	36	63	12	-5.2574
L preCUN	30	87	-6	-54	9	3.7329
L preCUN	-	83	-3	-63	36	4.2158
L SFG	32	44	-18	36	36	3.386
R SFG	32	54	15	39	39	4.521

CRBL: Cerebellum; ORB supmed: Superior frontal gyrus, medial orbital; SFG: Superior medial frontal gyrus; preCUN: Precuneus; MFG: Middle frontal gyrus; R: Right; L: Left; MNI: Montreal Neurological Institute; BA: Brodmann area.

in the ITG were observed in amblyopia patients^[23]. In humans, the STG is involved in emotion and sound processing^[24]. Therefore, the observed increased ALFF values for the HM group in the left ITG and left STG may imply cognitive compensations with regards to vision, emotion, and sound processing, due to HM. In this study, significantly increased ALFF values in the HM group were detected in the left ANG. Evidence has shown that the ANG is activated when the mind is at a resting state and is deactivated when the mind is engaged in cognitively demanding tasks^[25-26]. The ANG is involved in a number of processes related to language abilities, number processing, spatial cognition, memory retrieval, attention, and the theory of the mind^[27-28]. A recent study suggests that adolescents who have higher cognitive function scores (CFS) also have higher odds of having HM, especially for the verbal components of the cognitive function^[10]. Our results on ANG activation potentially support the finding regarding the verbal components of the cognitive function, however, it still needs to be confirmed by the subjective cognitive assessment.

Huang *et al*^[18] reported that significantly decreased ALFFs were found in the bilateral MTG, whereas we found significantly increased ALFFs in the right MTG. Compared to their study, we had a higher diopter of myopia, so we speculated that MTG may be impaired in HM with SE of -6.00 to -7.00 D, while in HM with higher diopter, MTG may undergo brain functional reorganization. Another functional study revealed decreased ALFFs in the bilateral REC of patients with low/moderate myopia^[19], whereas our results showed increased ALFFs in the bilateral REC of HM, we surmised that these changes might be associated with abnormal cognitive function due to HM.

DMN is considered as an important brain network closely related to advanced cognitive activities^[29]. Our study demonstrated that, compared with the non-HM group, the HM group showed greater FC in the PCC/preCUN and decreased FC in the mPFC. In general, the PCC/preCUN and mPFC are two important functional hubs in the DMN and are thought to be associated with emotional processing, such as attention and

the identification and regulation of emotion^[30-31]. Furthermore, the PCC/preCUN is considered to play an important role in the integration of visual information with spontaneous cognition^[32-33]. Based on the existing evidence, our findings suggest alterations in the emotional processing and visual integration among HM patients, which may further alter cognitive function.

ROI analyses revealed increased FC in the right PCC/preCUN in the HM group. Moreover, HM patients showed increased FC between the PCC/preCUN and the right CRBL and SFG, left preCUN, SFG, and ORB supmed and decreased FC in the right MFG. As a cognitive control, the PCC/preCUN plays a crucial role in monitoring the efficient allocation of attention to spatial behavior^[32,34], the SFG has been found to be involved in self-awareness and coordinating the activity of the sensory system^[35], and the MFG is involved in managing cognitive loads^[36]. Thus, the changes observed in the ROI analyses further revealed cognitive modifications among HM patients.

In our study, no abnormal functional changes in visual pathways were found. It may have something to do with the fact that we chose a more rigorous multiple comparison correction in ALFF. For the routine MRI examinations, there were a little spotted high intensity in the bilateral frontal white matter on the T2 weighted images for three patients of HM group, which were considered as non-characteristic changes, and the others of HM group and non-HM group were normal.

The primary limitations of our study are as follows: 1) The sample size for each diagnostic group was relatively small. There were following two reasons, one was patient recruitment, to avoid the potential effects due to different status of refractive correction, we only included HM patients with appropriate correction by wearing glasses, and excluded those with over or under refractive correction more than ± 1 D or wearing contact lens and receiving refractive surgery. The other is that MRI examinations in our study were time-consuming, so we excluded the patients who cannot complete the full examination. Studies with larger sample sizes are

necessary to verify and improve our results. 2) Although we found multiple characteristic changes among HM patients, which imply cognitive alterations due to HM, there is still a lack of correlation analysis between current results and CFS. Considering the complex networks among regions of the DMN, further investigation must be conducted to confirm our findings and determine corresponding clinical cognitive alterations through performing cognitive assessment. Currently, there are three cognitive assessment tests used for myopia, including Abbreviated Mental test^[7-8], Tower of London test^[9] and CFS^[10], however, the most valuable test for patients with HM needs further evaluation.

In summary, our data showed that neuroimaging alterations can be observed among HM patients compared with non-HM controls, supporting our hypothesis that HM patients have different ALFFs and DMNs which may result in cognitive alterations due to HM. However, because this is a preliminary study and phenomenological description, some of these results cannot be explained and great efforts must be made to achieve more comprehensive findings and to generate neuroimaging maps that can describe the full-scale cognitive characteristics associated with HM.

ACKNOWLEDGEMENTS

Foundations: Supported by the National Natural Science Foundation of China (No.81870685); Beijing Natural Science Foundation (No.7172173); Key Laboratory of Myopia, Ministry of Health (Fudan University) (No.EENTM-15-01).

Conflicts of Interest: Zhang XW, None; Dai RP, None; Cheng GW, None; Zhang WH, None; Long Q, None.

REFERENCES

- 1 Holden BA, Fricke TR, Wilson DA, Jong M, Naidoo KS, Sankaridurg P, Wong TY, Naduvilath TJ, Resnikoff S. Global prevalence of myopia and high myopia and temporal trends from 2000 through 2050. *Ophthalmology* 2016;123(5):1036-1042.
- 2 Morgan IG, French AN, Ashby RS, Guo XX, Ding XH, He MG, Rose KA. The epidemics of myopia: aetiology and prevention. *Prog Retin Eye Res* 2018;62:134-149.
- 3 Ikuno Y. Overview of the complications of high myopia. *Retina* 2017;37(12):2347-2351.
- 4 Abdolrahimzadeh S, Parisi F, Plateroti AM, Evangelista F, Fencicia V, Scuderi G, Recupero SM. Visual acuity, and macular and peripapillary thickness in high myopia. *Curr Eye Res* 2017;42(11):1468-1473.
- 5 Zhai LY, Li Q, Wang TY, Dong HH, Peng YM, Guo MX, Qin W, Yu CS. Altered functional connectivity density in high myopia. *Behav Brain Res* 2016;303:85-92.
- 6 Li Q, Guo MX, Dong HH, Zhang YT, Fu Y, Yin XH. Voxel-based analysis of regional gray and white matter concentration in high myopia. *Vis Res* 2012;58:45-50.
- 7 Sun HP, Liu H, Xu Y, Pan CW. Myopia and cognitive dysfunction among elderly Chinese adults: a propensity score matching analysis. *Ophthalmic Physiol Opt* 2016;36(2):191-196.
- 8 Ong SY, Ikram MK, Haaland BA, Cheng CY, Saw SM, Wong TY, Cheung CY. Myopia and cognitive dysfunction: the Singapore Malay eye study. *Invest Ophthalmol Vis Sci* 2013;54(1):799.
- 9 Mirshahi A, Ponto KA, Laubert-Reh D, Rahm B, Lackner KJ, Binder H, Pfeiffer N, Unterrainer JM. Myopia and cognitive performance: results from the Gutenberg health study. *Investig Ophthalmol Vis Sci* 2016;57(13):5230-5236.
- 10 Megreli J, Barak A, Bez M, Bez D, Levine H. Association of Myopia with cognitive function among one million adolescents. *BMC Public Heal* 2020;20:647.
- 11 Li K, Su W, Li SH, Jin Y, Chen HB. Resting state fMRI: a valuable tool for studying cognitive dysfunction in PD. *Park Dis* 2018;2018:6278649.
- 12 Pereira L, Airan RD, Fishman A, Pillai JJ, Kansal K, Onyike CU, Prince JL, Ying SH, Sair HI. Resting-state functional connectivity and cognitive dysfunction correlations in spinocerebellar ataxia type 6 (SCA6). *Hum Brain Mapp* 2017;38(6):3001-3010.
- 13 Lei H, Huang L, Li JX, Liu WT, Fan J, Zhang XC, Xia J, Zhao K, Zhu XZ, Rao HY. Altered spontaneous brain activity in obsessive-compulsive personality disorder. *Compr Psychiatry* 2020;96:152144.
- 14 Dai PS, Zhang JL, Wu J, Chen ZL, Zou BJ, Wu Y, Wei X, Xiao MY. Altered spontaneous brain activity of children with unilateral amblyopia: a resting state fMRI study. *Neural Plast* 2019;2019:1-10.
- 15 Anticevic A, Cole MW, Murray JD, Corlett PR, Wang XJ, Krystal JH. The role of default network deactivation in cognition and disease. *Trends Cogn Sci* 2012;16(12):584-592.
- 16 Putchá D, Ross RS, Cronin-Golomb A, Janes AC, Stern CE. Saliency and default mode network coupling predicts cognition in aging and Parkinson's disease. *J Int Neuropsychol Soc* 2016;22(2):205-215.
- 17 Zhang H, Zuo XN, Ma SY, Zang YF, Milham MP, Zhu CZ. Subject order-independent group ICA (SOI-GICA) for functional MRI data analysis. *NeuroImage* 2010;51(4):1414-1424.
- 18 Huang X, Zhou FQ, Hu YX, Xu XX, Zhou X, Zhong YL, Wang J, Wu XR. Altered spontaneous brain activity pattern in patients with high myopia using amplitude of low-frequency fluctuation: a resting-state fMRI study. *Neuropsychiatr Dis Treat* 2016;12:2949-2956.
- 19 Cheng Y, Huang X, Hu YX, Huang MH, Yang B, Zhou FQ, Wu XR. Comparison of intrinsic brain activity in individuals with low/moderate myopia versus high myopia revealed by the amplitude of low-frequency fluctuations. *Acta Radiol Stock Swed* 2020;61(4):496-507.
- 20 Hu YX, He JR, Yang B, Huang X, Li YP, Zhou FQ, Xu XX, Zhong YL, Wang J, Wu XR. Abnormal resting-state functional network centrality in patients with high myopia: evidence from a voxel-wise degree centrality analysis. *Int J Ophthalmol* 2018;11(11):1814-1820.
- 21 Wang JF, Chen HY, Liang HZ, Wang WM, Liang Y, Liang Y, Zhang YM. Low-frequency fluctuations amplitude signals exhibit abnormalities of intrinsic brain activities and reflect cognitive impairment in leukoaraiosis patients. *Med Sci Monit* 2019;25:5219-5228.

- 22 Liu WL, Yang J, Chen K, Luo CY, Burgunder J, Gong QY, Shang HF. Resting-state fMRI reveals potential neural correlates of impaired cognition in Huntington's disease. *Park Relat Disord* 2016;27:41-46.
- 23 Mendola JD, Conner IP, Roy A, Chan ST, Schwartz TL, Odom JV, Kwong KK. Voxel-based analysis of MRI detects abnormal visual cortex in children and adults with amblyopia. *Hum Brain Mapp* 2005;25(2):222-236.
- 24 Schirmer A, Gunter TC. Temporal signatures of processing voiceness and emotion in sound. *Soc Cogn Affect Neurosci* 2017;12(6):902-909.
- 25 Multani N, Taghdiri F, Anor CJ, Varriano B, Misquitta K, Tang-Wai DF, Keren R, Fox S, Lang AE, Vijverman AC, Marras C, Tartaglia MC. Association between social cognition changes and resting state functional connectivity in frontotemporal dementia, Alzheimer's disease, Parkinson's disease, and healthy controls. *Front Neurosci* 2019;13:1259.
- 26 Seghier ML. The angular gyrus: multiple functions and multiple subdivisions. *Neurosci* 2013;19(1):43-61.
- 27 Faye A, Jacquin-Courtois S, Reynaud E, Lesourd M, Besnard J, Osiurak F. Numerical cognition: a meta-analysis of neuroimaging, transcranial magnetic stimulation and brain-damaged patients studies. *Neuroimage Clin* 2019;24:102053.
- 28 Igelström KM, Graziano MSA. The inferior parietal lobule and temporoparietal junction: a network perspective. *Neuropsychologia* 2017;105:70-83.
- 29 Broyd SJ, Demanuele C, Debener S, Helps SK, James CJ, Sonuga-Barke EJS. Default-mode brain dysfunction in mental disorders: a systematic review. *Neurosci Biobehav Rev* 2009;33(3):279-296.
- 30 Soch J, Deserno L, Assmann A, Barman A, Walter H, Richardson-Klavehn A, Schott BH. Inhibition of information flow to the default mode network during self-reference versus reference to others. *Cereb Cortex* 2017;27(8):3930-3942.
- 31 Li Q, Zhang B, Cao H, Liu W, Guo F, Shen FY, Ye BL, Liu H, Li Y, Liu ZQ. Oxytocin exerts antidepressant-like effect by potentiating dopaminergic synaptic transmission in the mPFC. *Neuropharmacology* 2020;162:107836.
- 32 Leech R, Smallwood J. The posterior cingulate cortex: insights from structure and function. *Handb Clin Neurol* 2019;166:73-85.
- 33 Leech R, Sharp DJ. The role of the posterior cingulate cortex in cognition and disease. *Brain* 2014;137(1):12-32.
- 34 Leech R, Kamourieh S, Beckmann CF, Sharp DJ. Fractionating the default mode network: distinct contributions of the ventral and dorsal posterior cingulate cortex to cognitive control. *J Neurosci* 2011;31(9):3217-3224.
- 35 Hashimoto R, Ikeda M, Yamashita F, Ohi K, Yamamori H, Yasuda Y, Fujimoto M, Fukunaga M, Nemoto K, Takahashi T, Tochigi M, Onitsuka T, Yamasue H, Matsuo K, Iidaka T, Iwata N, Suzuki M, Takeda M, Kasai K, Ozaki N. Common variants at 1p36 are associated with superior frontal gyrus volume. *Transl Psychiatry* 2014;4(10):e472.
- 36 Li X, Wang WX, Wang AL, Li P, Zhang JY, Tao WH, Zhang ZJ. Vulnerability of the frontal and parietal regions in hypertensive patients during working memory task. *J Hypertens* 2017;35(5):1044-1051.